http://doi.org/10.35784/iapgos.7465 *received: 22.03.2025 | revised: 30.05.2025 | accepted: 05.03.2026 | available online: 30.06.2026*

OPTIMISATION OF THE GENERATING CAPACITY OF DROOP-BASED DGs INTEGRATED INTO AN ISOLATED AC MICROGRID USING METAHEURISTIC ALGORITHMS TO MINIMISE POWER LOSSES

Tuan-Ho Le[1], Tham X. Nguyen[1], Robert Lis[2], Muhammad Jamshed Abbass[2]
[1]Quy Nhon University, Faculty of Engineering and Technology, Quy Nhon, Vietnam, [2]Wrocław University of Science and Technology, Faculty of Electrical Engineering, Wrocław, Poland

Abstract. *This study proposes three metaheuristic techniques, including differential evolution, moth-flame optimisation, and honey badger algorithm combined with a modified backward-forward sweep load flow approach to identify the optimal droop gains and reference voltage magnitudes of distributed generators (DGs) (i.e., optimal size of droop-based DGs) integrated with renewable sources to meet the electricity demands of an islanded AC microgrid. The suggested mathematical model was tested on a reconfigured 33-bus islanded microgrid under four scenarios with a time-varying load over 24 hours. The findings indicate that Case 3, which applies the honey badger (HB) algorithm to optimise droop coefficients and regulate reference voltage magnitudes within permissible limits, is the most effective in lowering power losses compared to other cases. The final results highlight the HB algorithm's efficacy in minimising power losses while optimising the size of droop-based DGs in an islanded microgrid integrated with renewable energy sources.*

Keywords: islanded AC microgrid, losses power minimisation, voltage improvement, metaheuristic algorithms

OPTYMALIZACJA ZDOLNOŚCI WYTWÓRCZYCH GENERATORÓW ROZPROSZONYCH Z REGULOWANYM STATYZMEM ZINTEGOWANYCH W IZOLOWANEJ MIKROSIECI AC PRZY WYKORZYSTANIU ALGORYTMÓW METAHEURYSTYCZNYCH W CELU ZMNIEJSZENIA STRAT SIECIOWYCH

Streszczenie. *W niniejszym badaniu zaproponowano trzy techniki metaheurystyczne, obejmujące algorytm ewolucji różnicowej (ang. Differential Evolution – DE), optymalizację Moth-Flame (MFO) oraz algorytm Honey Badger (HB), połączone ze zmodyfikowaną metodą rozpływu mocy i napięć (ang. Modified Backward-Forward Sweep – MBFS), w celu optymalnego planowania punktu pracy generatorów rozproszonych (DG) z regulowanym statyzmem w rozwiniętej strukturze hierarchicznej izolowanej mikrosieci prądu przemiennego (AC). Take algorytmy sterowania sprawiają, że generatory DG same mogą regulować napięcie mikrosieci, podczas gdy pracuje ona w trybie wyspowym. Zaproponowany model matematyczny został przetestowany na rekonfigurowanej izolowanej mikrosieci 33-węzłowej w czterech scenariuszach, z obciążeniem zmieniającym się w ciągu doby. Wyniki wskazują, że scenariusz 3, w którym zastosowano algorytm HB do optymalizacji wartości współczynników quasi-stacjonarnego odchylenia napięcia oraz regulacji wartości napięcia referencyjnego w dopuszczalnych granicach, jest najbardziej efektywny do obniżenia strat mocy i energii w porównaniu do innych przypadków. W szczególności, w scenariuszu 3, w którym zastosowano algorytm HB, straty mocy czynnej i biernej odpowiednio stanowią jedynie 0.9459% i 1.1485% całkowitego zapotrzebowania na moc. Wyniki te podkreślają skuteczność algorytmu HB w minimalizacji strat mocy przy jednoczesnej optymalizacji rozmiaru DG opartych na regulowanym statyźmie w testowej mikrosieci, pracującej w trybie wyspowym.*

Słowa kluczowe: wyspowa mikrosieć AC, minimalizacja strat mocy, poprawa napięcia, algorytmy metaheurystyczne

Introduction

Small-scale dispersed and distributed generators (DG) are increasingly favoured for deployment in distribution networks, particularly in microgrids. A microgrid can exchange energy with the national power system through a point of coupling, operating in grid-connected mode. Alternatively, it can function independently, supplying its own energy needs in grid-off mode, also known as islanded mode. Islanded operation offers significant advantages and aligns with the future development of power grids [7, 26]. To mitigate environmental concerns associated with fossil fuel-based generators, integrating multiple renewable DGs of varying capacities and types into microgrids is crucial. However, this integration poses challenges, especially in optimising the placement and sizing of DGs. This study explores the deployment of appropriately sized, droop-controlled, renewable-based DGs in an islanded AC microgrid.

Various techniques have been introduced to determine the optimal size of an islanded/isolated/standalone microgrid, including metaheuristic algorithms [3, 10, 20, 21], hybrid techniques [14, 17, 19, 28], multi-objective optimisation methods [8, 12, 15, 23], mixed-integer linear programming (MILP) technique [2, 11], hybrid optimisation of multiple energy resources (HOMER) tool [16], and general algebraic modelling (GAMS) system [3].

The proper capacity of a backup energy storage device (BESD) within a standalone microgrid integrating a solar photovoltaic (PV) plant has been found using particle swarm optimisation (PSO) algorithm to maintain grid frequency inside predetermined limits [10]. In [3], researchers developed grey wolf optimisation approach to size the BESD in an islanded microgrid (IMG) on Flinders Island, Australia, aiming to support frequency stability. Differential evolution (DE) technique [21] and honey badger (HB) algorithm [20] have been proposed to optimise the allocation of droop-based DGs for minimising power losses.

In [28], the locations and capacities of wind turbines (WT), diesel-based DGs, and capacitor banks (CB) in IMGs with high nonlinear load penetration are determined using genetic algorithm (GA) and mixed-integer nonlinear programming (MINLP) techniques to minimise total costs. In [14], a combination of the GA toolbox and an efficient optimisation method known as the sensitivity region (SR) is developed to find the hosting capacity of droop-regulated and renewable-based IMGs, aiming to reduce frequency deviations due to the uncertainty of renewable DG. A hybrid approach combining GA and PSO is proposed in [17] to optimise the sizing of WT, solar PV, battery, fuel cell, and hydrogen tank for electricity supply on a Mediterranean island. In [19], an advanced hybrid technique integrating GA, PSO, and MINLP is developed to optimise the planning and allocation of remote microgrids, ensuring reliable electricity supply while minimising annualized capital and operational costs.

The planning of droop and renewable-based IMGs is optimised using multi-objective ant lion optimisation (MALO) algorithm to minimise investment costs while accounting for the uncertainty of renewable generation [8]. The search algorithm referencing adjacent points (SARAP) is introduced to determine the optimal capacities of WT, solar PV system, diesel generator, and battery storage in a standalone microgrid, aiming to lower annual costs and emissions [15]. In [23], losses power and operational costs in a droop-based IMG are minimised using a multi-objective PSO algorithm to find the suitable sizing of droop-regulated DGs, renewable DGs, and CBs. The efficient non-dominated sorting genetic algorithm-II (NSGA-II) is proposed in [12] to determine the optimal capacity of IMGs

integrating renewable-rich DGs, considering battery storage device and fuel cell development to meet load demand under renewable generation and load variations over time.

The MILP technique is suggested to identify the appropriate capacity of IMGs for effective techno-economic planning [11], economic and environment optimisation [2]. Ref. [16], the ideal size of WT, PV, hydrokinetic turbine, and battery system is obtained through the HOMER tool to meet the electric demand of the Persian Gulf Islands. GAMS software is applied to get the optimal battery capacity for a microgrid functioning in both grid-off and islanded modes with the integration of wind energy [24].

According to researchers D.H. Wolpert and W.G. Macready in [27], no single algorithm can provide a perfect solution to every optimisation issue. In this study, three metaheuristic techniques including DE, moth-flame optimisation (MFO), and HB are developed to identify the appropriate capacity of droop-based DGs integrated with renewable DGs within an islanded AC microgrid, with the aim of mitigating losses power and improving nodal voltage.

This work is presented as follows. The first section is Introduction part. Problem formulation and constraint conditions are presented in sections 2 and 3 respectively. The fourth section describes Proposed solution. Subsequently, Data and cases are expressed. The sixth section shows Results and discussion. The last section includes Conclusion and future work.

1. Problem formulation

The main priority is to minimise the active power loss F_1 for the droop-based islanded microgrid (DIMG) grid, while accounting for the reactive power loss F_2.

$$\min F_1(\boldsymbol{x}_S,\ \boldsymbol{x}_{Vref}) \tag{1}$$

$$\boldsymbol{x}_S = [m_{p1}, m_{p2}, ..., m_{pi}, n_{q1}, n_{q2}, ..., n_{qi}],\ i \in [1, N_{DDG}] \cap Z$$

$$\boldsymbol{x}_{Vref} = [\,|V_{ref\,1}|, |V_{ref\,2}|, ..., |V_{refi}|\,],\ i \in [1, N_{DDG}] \cap Z$$

where $\boldsymbol{x}_S$ and $\boldsymbol{x}_{Vref}$ are the vectors of droop gains and reference voltage magnitude of the droop-based distributed generators (DDG) respectively; m_{pi} denotes the real power droop coefficient of the *i*-th DDG, while n_{qi} signifies the reactive power droop gain; $|V_{refi}|$ is the reference voltage magnitude of the DDG *i;* N_{DDG} represents the number of DDGs injecting power into the grid; Z is a numerical integer.

The real and reactive power losses in the radial branches of islanded AC microgrids can be determined as follows:

$$F_1 = \sum_{t=1}^{T}\sum_{h=1}^{N} R_h I_h^2 \tag{2}$$

$$F_2 = \sum_{t=1}^{T}\sum_{h=1}^{N} X_h I_h^2 \tag{3}$$

where the resistance of branch h is R_h, its reactance is X_h, and the current through it is represented by I_h; N denotes the number of branches of the network; T represents the full period of investigation.

2. Constraint conditions

a. Power balance equations

The power produced by all DGs and injected into load buses at time t is described as follows:

$$\left(\sum_{i=1}^{N_{DDG}} \frac{1}{m_{pi}}\left(f(t) - f_{ref}\right) + \sum_{i=1}^{N_{DDG}} P_{DGio}\right) + \sum_{k=1}^{N_{WT}} P_{WTk}(t) + \sum_{k=1}^{N_{PV}} P_{PVk}(t) \tag{4}$$

$$-\sum_{n=1}^{N_L} P_{Ln}(t) = \sum_{n=1}^{N_L}\sum_{m=1}^{N_L} |V_n(t)||V_m(t)||Y_{nm}(t)|\cos\left(\delta_n(t) - \delta_m(t) - \theta_{nm}(t)\right)$$

$$\left(\sum_{i=1}^{N_{DDG}} \frac{1}{n_{qi}}\left(|V_i(t)| - |V_{refi}(t)|\right) + \sum_{i=1}^{N_{DDG}} Q_{DGio}\right) - \sum_{n=1}^{N_L} Q_{Ln}(t) \tag{5}$$

$$= \sum_{n=1}^{N_L}\sum_{m=1}^{N_L} |V_n(t)||V_m(t)||Y_{nm}(t)|\sin\left(\delta_n(t) - \delta_m(t) - \theta_{nm}(t)\right)$$

where $f(t)$ is used to indicate the operating frequency at time *t*, and f_{ref} stands for the reference frequency; the reference production powers of the DDG i are represented by P_{DGio} and Q_{DGio}; $P_{Ln}(t)$ and $Q_{Ln}(t)$ are electric load demand of the *n*-th bus at time *t*; $|V_i(t)|$, $|V_n(t)|$ and $|V_m(t)|$ are the operating voltage magnitudes, while $\delta_n(t)$ and $\delta_m(t)$ are their phase angles; $|Y_{nm}(t)|$ is the magnitude of the branch admittance between two nodes *n* and *m*, while $\theta_{nm}(t)$ denotes its phase angle; $P_{WTk}(t)$ is the production power of the *k*-th wind turbine at time *t*; $P_{PVk}(t)$ represents the produced power of the *k*-th solar PV plant at time *t*; N_{WT} and N_{PV} are the number of wind turbines and solar PV plants respectively; N_L is the number of the DIMG buses.

b. Inequality constraints

b.1. The frequency and voltage magnitude of the DIMG network

$$\omega^{\min} \le \omega(t) \le \omega^{\max} \tag{6}$$

$$|V^{\min}| \ \le\ |V_n(t)|\ \le\ |V^{\max}|,\ n \in [1, N_L] \cap Z \tag{7}$$

where $\omega^{\max}$ and $\omega^{\min}$ are the top and bottom thresholds of the DIMG frequency respectively; $|V^{\max}|$ and $|V^{\min}|$ signify the upper and lower limits of the bus voltage magnitude; in this study, $\omega^{\max}$ and $\omega^{\min}$ are predetermined 1.0 pu and 0.99 pu respectively, while $|V^{\max}|$ and $|V^{\min}|$ are given 1.05 pu and 0.95 pu.

b.2. Power limit of droop-based distributed generators

$$0 \le P_{DDGi}(t) \le P_{DDGi}^{\max},\ i \in [1, N_{DDG}] \cap Z \tag{8}$$

$$0 \le Q_{DDGi}(t) \le Q_{DDGi}^{\max},\ i \in [1, N_{DDG}] \cap Z \tag{9}$$

where P_{DDGi} and Q_{DDGi} are the production powers of the DDG *i* at time *t*; $P_{DDGi}^{\max}$ and $Q_{DDGi}^{\max}$ denote the top limits of the production powers of the *i*-th DDG.

b.3. The reference voltage magnitude and droop coefficients of droop-based distributed generators

$$|V_{ref}^{\min}| \ \le\ |V_{refi}(t)|\ \le\ |V_{ref}^{\max}|,\ i\ \in [1, N_{DDG}] \cap Z \tag{10}$$

$$m_{pi}^{\min} \le m_{pi}(t) \le m_{pi}^{\max},\ i\ \in [1, N_{DDG}] \cap Z \tag{11}$$

$$n_{qi}^{\min} \le n_{qi}(t) \le n_{qi}^{\max},\ i\ \in [1, N_{DDG}] \cap Z \tag{12}$$

where $|V_{ref}^{\min}|$ and $|V_{ref}^{\max}|$ are the lower and upper limits of the reference voltage magnitude of the DDG *i* with their values predetermined as 1.0 pu and 1.02 pu respectively, in this study; $m_{pi}^{\min}$ and $m_{pi}^{\max}$ represent the bottom and top limits of the real droop gain of the *i*-th DDG, while $n_{qi}^{\min}$ and $n_{qi}^{\max}$ denote the bottom and top thresholds of the reactive droop coefficient.

b.4. Power threshold of renewable DGs

$$P_{PVk}^{\min}\ \le\ P_{PVk}(t)\ \le\ P_{PVk}^{\max} \tag{13}$$

$$P_{WTk}^{\min}\ \le\ P_{WTk}(t)\ \le\ P_{WTk}^{\max} \tag{14}$$

where $P_{PVk}^{\min}$ and $P_{PVk}^{\max}$ indicate the produced power thresholds of solar PV plant *k*, while $P_{WTk}^{\min}$ and $P_{WTk}^{\max}$ are the power limits provided by wind turbine *k*.

3. Proposed solution

Three metaheuristic algorithms consist of the DE, MFO, and HB along with the modified backward-forward sweep load flow approach proposed by Hameed F. et al in 2017 [5] are applied to determine the proper capacity of DDGs integrating renewable DGs within the islanded AC microgrid. The suggested methodologies are described as follows:

a.1. DE-based metaheuristic technique

Price and Storn introduced the DE technique in 1995 [22]. This population-based optimisation method is widely used to find optimal solutions in various technical applications.

The DE algorithm is conducted through four steps, namely, initialisation, mutation, crossover, and selection. The initialisation step uses random technique to generate the initial population:

$$X_{ij} = BB_j + \text{rand}_j(0,1)(TB_j - BB_j),\ i \in [1, N_{DE}] \cap Z,\ j \in [1, D_{DE}] \cap Z$$

where BB_j is the bottom limit of the j-th adjustable variable, while TB_j denotes its top threshold. N_{DE} represents the number of inhabitants within the population, and D_{DE} is the dimensional vectors of the adjustable variables, Z describes a numerical integer.

The mutation step is to enhance solution diversity within the population. It can be performed by: $\boldsymbol{V}_i^g = \boldsymbol{X}_{s3}^g + F(\boldsymbol{X}_{s1}^g - \boldsymbol{X}_{s2}^g)$, $i \in [1, N_{DE}] \cap Z, g \in [1, G_{\max}] \cap Z$, where $\boldsymbol{V}_i^g$ is the mutant vector in the generation g, while $\boldsymbol{X}_{s1}^g$, $\boldsymbol{X}_{s2}^g$ and $\boldsymbol{X}_{s3}^g$ are the solution vectors in the population at the generation g, F is the scaling factor, $G_{\max}$ is the maximum generation count, s_1, s_2 and s_3 signify different positive integer indices chosen randomly.

The crossover mechanism is used to generate new population in the g-th generation, it can be expressed by the following equation:

$$U_{ij}^g = \begin{cases} V_{ij}^g & \text{if } r_j(0,1) \le CR_{DE} \text{ or } j \in [1, D_{DE}] \cap Z \\ X_{ij}^g & \text{otherwise} \end{cases}$$

where CR_{DE} denotes the crossover factor, $r_j(0, 1)$ represents a uniformly distributed random value.

The selection step is to find the optimal solution at the generation g. When resolving a minimal problem, the corresponding solution with the best value (lowest) of the objective function is determined and described by

$$\boldsymbol{X}_i^g = \begin{cases} \boldsymbol{U}_i^g & \text{if } f(\boldsymbol{U}_i^g) \le f(\boldsymbol{X}_i^g) \\ \boldsymbol{X}_i^g & \text{otherwise} \end{cases}, f() \text{ is the objective function}$$

a.2. MFO-based metaheuristic technique

The MFO algorithm was originally proposed by the researcher Mirjalili in 2015 [18]. It mimics the behaviour of moths, which use a logarithmic spiral flight to move toward light sources. In the algorithm, moths represent candidate solutions, while flames act as guiding points (best solutions). Moths update their positions based on a spiral movement around flames, gradually refining their solutions. The MFO technique is widely used for solving complex optimisation problems due to its strong exploration and exploitation capabilities.

The following expresses a pseudo code of the MFO technique.

Pseudo code of MFO technique

Set parameters of MFO: $K_{\max}$, N, and D.
Establish an initial population M by randomly assigning Moths.
Evaluate each Moth m_i based on the objective function OM_i.
while stopping criteria are not met **do**
  Compute the number of local solutions nF using Eq. (15).
  if $k == 1$ **then**
    $F = sort(M)$, F: Flame matrix
    $OF = sort(OM)$, OF: Flame fitness matrix
  else
    $F = sort(M_{r-1}, M_r)$
    $OF = sort(M_{r-1}, M_r)$
  end
  for $i = 1$ to N **do**
    for $j = 1$ to D **do**
      Compute convergence constant a using Eq. (16).
      Compute r using Eq. (17).
      Determine D_i using Eq. (18).
      Update Moth position using Eq. (19).
    end
  end
end

$$nF = Int\left(N - \frac{k(N-1)}{K_{\max}}\right) \quad (15)$$

$$a = -\frac{k}{K_{\max}} - 1 \quad (16)$$

$$r = (a-1)rand + 1 \quad (17)$$

$$D_i = \left|F_j - M_i\right| \quad (18)$$

$$M_i = F_j + D_i e^{br} \cos 2\pi r \quad (19)$$

where $K_{\max}$ is the maximum iteration count, N represents the number of moths, D denotes the dimensional vectors of the control variables.

a.3. HB-based metaheuristic technique

The HB technique was first put forward by Hashim et al. in 2022 [6]. The HB algorithm is based on the behaviour of honey badgers in nature. It mimics their intelligent hunting strategies, including digging and honey techniques, to explore and exploit search spaces effectively. The HB is extensively applied to address real-world optimisation problems.

Below presents a pseudo code of the HB technique.

Pseudo code of HB technique

Set parameters: $T_{\max}$, N_{HB}, β, and C.
Generate the initial population with randomly assigned positions.
Evaluate each HB's placement z_i based on the objective function and allocate the computed fitness value to f_i, $i \in [1, N_{HB}] \cap Z$.
Save and allocate the best fitness to f_{prey}, and its position to z_{prey}.
while stopping criteria are not met **do**
  Compute the new value of α using Eq. (20).
  for $i = 1$ to N_{HB} **do**
    Determine the intensity of I_i using Eq. (21).
    if $r < 0.5$ **then**
      Compute the new placement $z_{i,update}^t$ using Eq. (22).
    else
      Compute the new placement $z_{i,update}^t$ using Eq. (23).
    end
    Evaluate the new placement and allocate to f_{update}.
    if $f_{update} \le f_i$ **then**
      Set $z_i^t = z_{i,update}^t$ and $f_i = f_{update}$.
    end
    if $f_{update} \le f_{prey}$ **then**
      Set $z_{prey} = z_{i,update}^t$ and $f_{prey} = f_{update}$.
    end
  end
end
return f_{prey} and z_{prey}.

$$\alpha = Ce^{-\frac{t}{T_{\max}}},\ t \in [1, T_{\max}] \cap Z \quad (20)$$

$$I_i = r_2 \frac{S}{4\pi d_i^2} \quad (21)$$

$$z_{i,update}^t = z_{prey} + F\beta l_i z_{prey} + Fr_3 \alpha d_i \left|\cos 2\pi r_4 [1 - \cos(2\pi r_5)]\right| \quad (22)$$

$$z_{i,update}^t = z_{prey} + Fr_7 \alpha d_i \quad (23)$$

a.4. Power flow method in an islanded microgrid

To maximise the benefits of deploying DGs in a microgrid, small-sized DGs are often preferred. Therefore, a slack bus does not exist in the islanded mode of the microgrid. In this work, the method described by Hameed F. et al. in 2017 [5] is employed to determine the power flow in the islanded microgrid.

4. Data and cases

The 33-bus DIMG grid is used in this work, as illustrated in Fig. 1. The topology of this network was reconfigured by isolating the tie-switch link connecting bus 1 to the primary grid substation from the standard network [1]. The rated real power load of the grid is 3.715 MW, while its rated reactive power is 2.3 MVAr, and the rated voltage is 12.66 kV. The droop-based DGs use diesel generators to provide the electricity for loads. Table 1 displays the suitable placement of DGs for four suggested cases. Table 2, Table 3, and Table 4 show the parameter setting of the DE, MFO, and HB algorithms respectively. The production power thresholds of three DDGs are described in Table 5. The model of the constant power load is employed together with the sensitivity parameters K_{pf} and K_{qf} in ref. [13] were set to zero. For three DDGs, the power reference points P_{DGio} and Q_{DGio} were determined to be 0.2 pu. The load profile was investigated over a 24-hour interval, as illustrated in Fig. 2 [25].

In Case 2, one solar PV DG with a rated capacity 500 kW was installed at the *25*-th bus. In Case 3, one WT DG with a rated size 500 kW was deployed at the *24*-th bus. In Case 4, both one WT DG and one PV DG were deployed at the buses 24 and 25, with capacities of 250 kW each respectively. Assume that the optimal positioning of DGs for Cases in the 33-bus DIMG network is described as in Table 1.

In order to evaluate the efficacy of three suggested meta-heuristic algorithms including DE, MFO, and HB for the optimal capacity of DDGs considering the integration of renewable DGs in the 33-bus DIMG network, four cases are selected as follows:
Case 1: only optimise the size of three DDGs
Case 2: optimise the size of three DDGs integrating one solar PV DG
Case 3: optimise the size of three DDGs integrating one WT DG
Case 4: optimise the size of three DDGs integrating one WT DG and one solar PV DG.

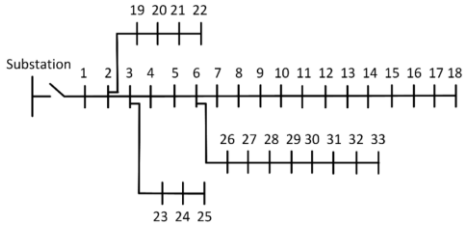

Fig. 1. The IEEE 33-bus IMG network

Table 1. Proper positioning of DGs for cases

Cases	DDG1 (bus)	DDG2 (bus)	DDG3 (bus)	PV (bus)	WT (bus)
1 [9]	2	12	26		
2 [9]	2	12	26	25	
3	2	12	26		24 [23]
4	2	12	26	25	24 [23]

Table 2. Settings of predefined parameters of the DE algorithm

Cases	$G_{\max}$	N_{DE}	F	CR	D_{DE}
1	100	100	0.2	0.5	9
2	100	100	0.2	0.5	9
3	100	100	0.2	0.5	9
4	100	100	0.2	0.5	9

Table 3. Settings of predefined parameters of the MFO

Cases	$K_{\max}$	N	b	D
1	100	100	1	9
2	100	100	1	9
3	100	100	1	9
4	100	100	1	9

Table 4. Settings of predefined parameters of the HB

Cases	$T_{\max}$	N_{HB}	β	C	D_H
1	100	100	6	2	9
2	100	100	6	2	9
3	100	100	6	2	9
4	100	100	6	2	9

Table 5. Active and reactive power thresholds of DDGs for cases

No. DDG	$P_{DDGi}^{\max}$ (kW)	$Q_{DDGi}^{\max}$ (kVAr)
DDG1	1650	1100
DDG2	1300	800
DDG3	950	640

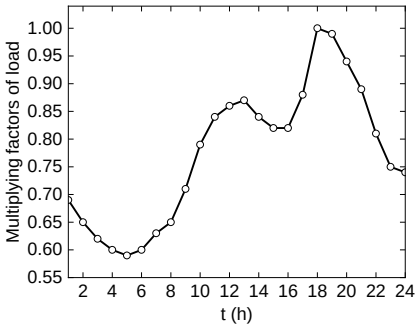

Fig. 2. Profile of load

5. Results and discussion

The problem of the optimal capacity of the DDGs integrating renewable DGs in the DIMG grid was scripted through MATLAB 2021a software. The experiment was carried out on a computer with a Core i7-9700 CPU, 3.0 GHz processor, and 16 GB of RAM to identify the proper values. To ensure the reliability of the results, each case was independently executed 40 times on the machine, using the proposed values for three algorithms.

Figs. 3–6 show the tuned values of the droop coefficients (m_{pi} and n_{qi}), and the reference voltage value $|V_{refi}|$ for three DDGs in four cases using the DE, MFO, and HB techniques corresponding to the investigated load profile in 24-h. These values are variables expressed in the Problem formulation section.

The working frequency of the 33-bus DIMG grid at the rated load using the suggested techniques is shown in Table 6, along with the frequency values at other load levels in this study that satisfy the predefined constraints.

Table 7 and Table 8 display the nominal powers of three DDGs for cases, determined from the tuned values m_{pi}, n_{qi} and $|V_{refi}|$ by each technique under rated load conditions.

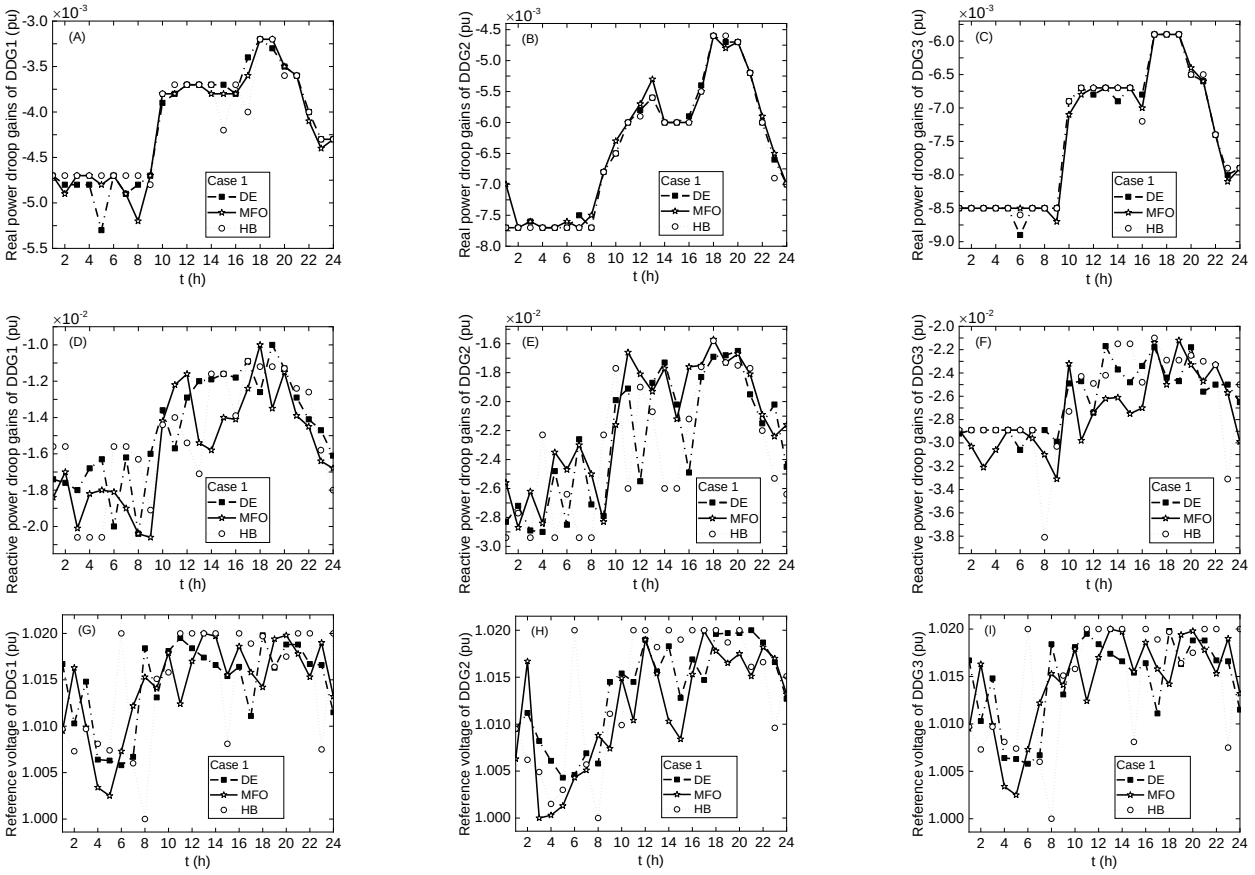

Fig. 3. Tuning m_{pi}, n_{qi} and $|V_{refi}|$ parameters of three DDGs for Case 1 m_{pi} of DDGs 1–3 (A-C), n_{qi} of DDGs 1–3 (D-F), and $|V_{refi}|$ of DDGs 1–3 (G-I)

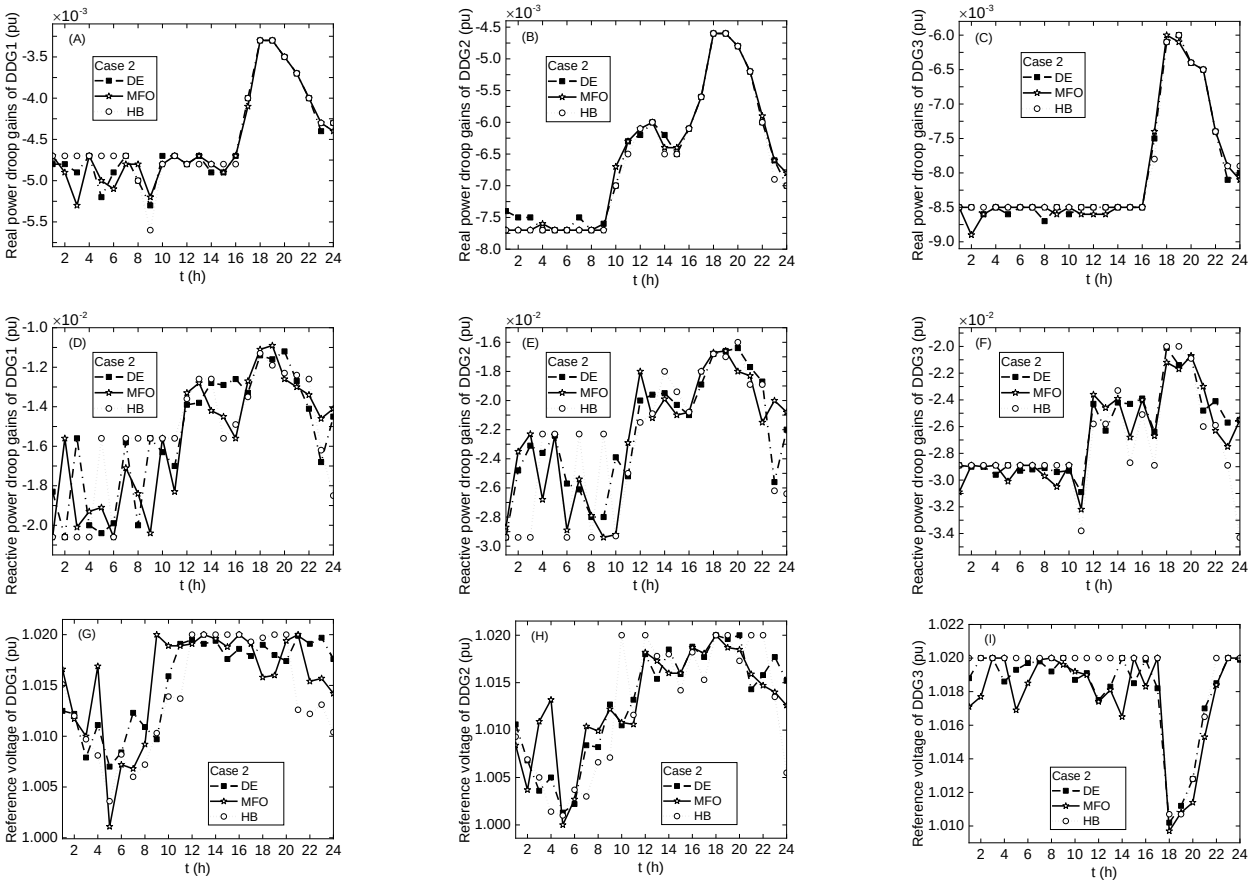

Fig. 4. Tuning m_{pi}, n_{qi} and $|V_{refi}|$ parameters of three DDGs for Case 2: m_{pi} of DDGs 1–3 (A-C), n_{qi} of DDGs 1–3 (D-F), and $|V_{refi}|$ of DDGs 1–3 (G-I)

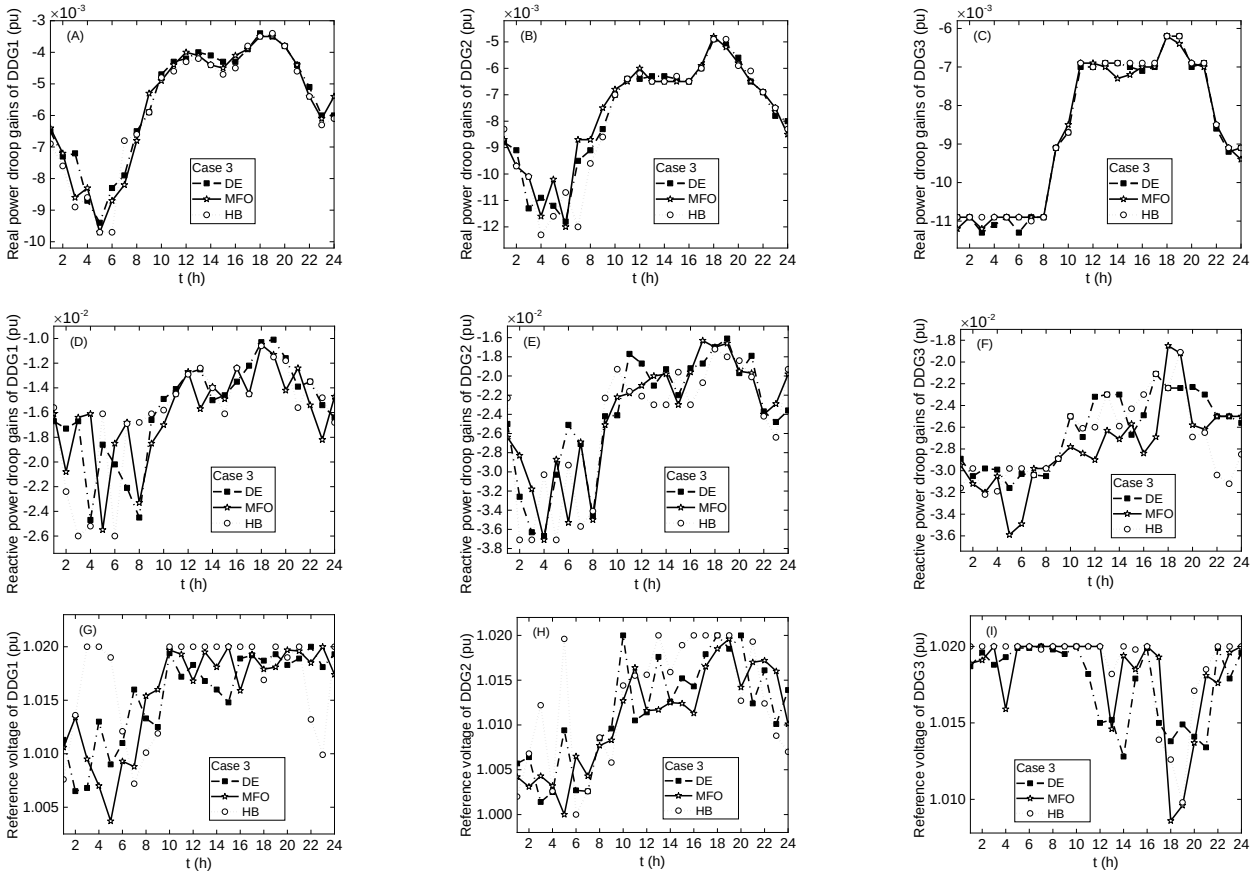

Fig. 5. Tuning m_{pi}, n_{qi} and $|V_{refi}|$ parameters of three DDGs for Case 3: m_{pi} of DDGs 1–3 (A-C), n_{qi} of DDGs 1–3 (D-F), and $|V_{refi}|$ of DDGs 1–3 (G-I)

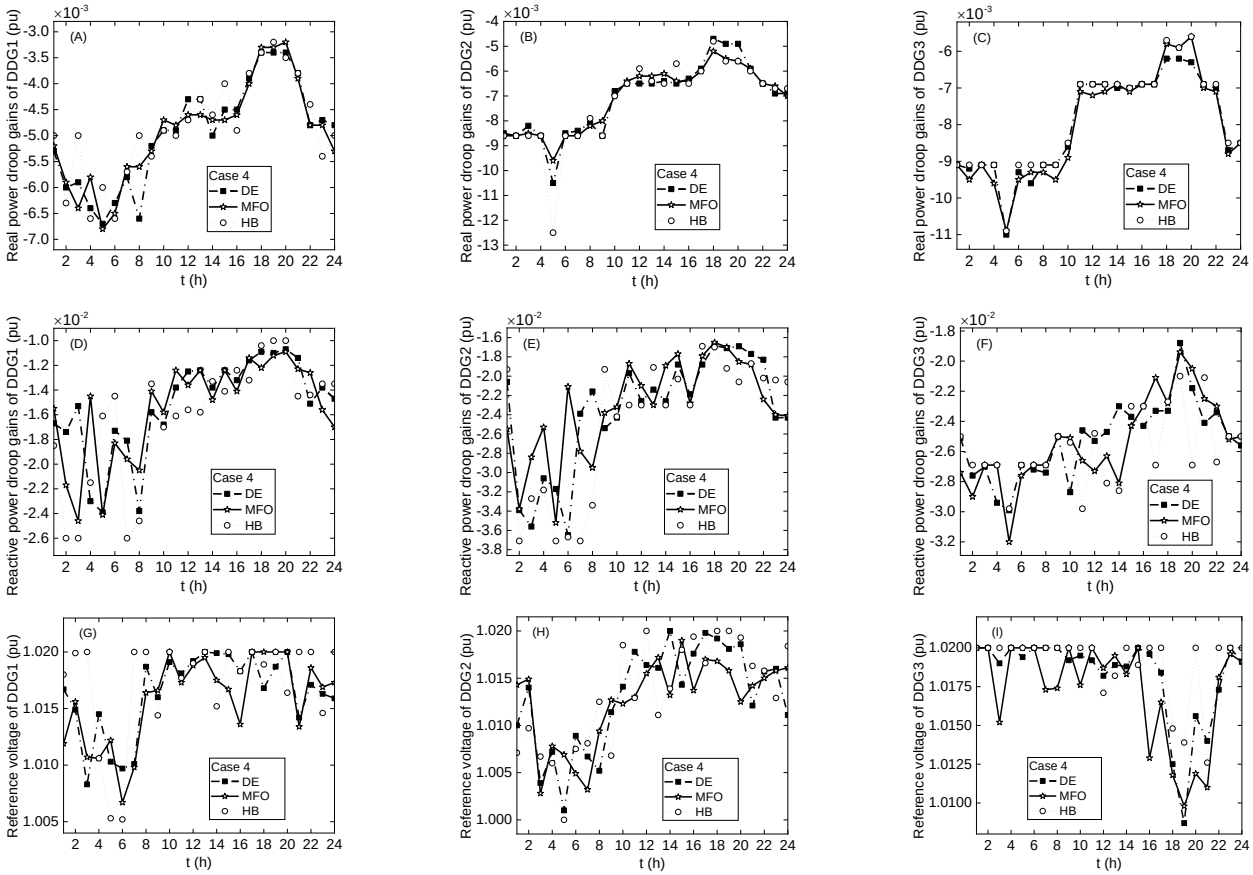

Fig. 6. Tuning m_{pi}, n_{qi} and $|V_{refi}|$ parameters of three DDGs for Case 4: m_{pi} of DDGs 1–3 (A-C), n_{qi} of DDGs 1–3 (D-F), and $|V_{refi}|$ of DDGs 1–3 (G-I)

Table 6. Frequency values (pu) of the DIMG at the rated load

Cases	1	2	3	4
MFO	0.9901	0.9902	0.9901	0.9902
DE	0.9901	0.9902	0.9902	0.9901
HB	0.9900	0.9902	0.9901	0.9903

Table 7. Rated active power of three DDGs

Cases	Algorithms	DG1 (kW)	DG2 (kW)	DG3 (kW)	Sum (kW)
1	MFO	1643.45	1191.65	935.65	3770.75
	DE	1648.35	1185.00	937.15	3770.50
	HB	1636.75	1187.75	945.70	3770.20
2	MFO	1572.30	1170.90	919.60	3662.80
	DE	1582.90	1170.45	909.30	3662.65
	HB	1591.15	1169.75	901.70	3662.60
3	MFO	1529.25	1120.90	890.25	3540.40
	DE	1542.25	1107.00	890.90	3540.15
	HB	1531.15	1110.65	898.50	3540.30
4	MFO	1600.50	1050.40	949.50	3600.40
	DE	1553.05	1150.60	898.00	3601.65
	HB	1531.80	1118.75	950.00	3600.55

Table 8. Rated reactive power of three DDGs

Cases	Algorithms	DG1 (kVAr)	DG2 (kVAr)	DG3 (kVAr)	Sum (kVAr)
1	MFO	1088.55	609.80	633.95	2332.30
	DE	1086.85	611.25	639.40	2337.50
	HB	1099.25	592.05	639.95	2331.25
2	MFO	1059.75	639.15	637.15	2336.05
	DE	1092.45	605.35	637.95	2335.75
	HB	1100.00	596.25	639.65	2335.90
3	MFO	1094.35	592.45	640.00	2326.80
	DE	1090.50	603.05	635.10	2328.65
	HB	1063.35	625.05	639.95	2328.35
4	MFO	1078.80	619.95	629.65	2328.40
	DE	1083.95	617.50	636.10	2337.55
	HB	1100.00	589.70	638.80	2328.50

Table 9 outlines the comparison of objective functions, including total real and reactive power losses and their percentages, for four cases evaluated using three suggested algorithms. According to ref. [14], the real power loss in islanded microgrids should remain below 1.5% of the rated load level. The numerical results in Table 9 indicate that the lowest power losses and loss percentages were achieved in Case 3 using the HB technique, while Case 1 with the MFO algorithm produced the highest losses. This outcome is attributed to the proper placement and sizing of DGs in Case 3, which involved optimising the size of three DDGs and integrating one WT DG, as compared to the other cases under the investigated load profile.

Table 9. Objective functions (P_{loss} and Q_{loss} are the real and reactive power losses respectively)

Cases	Algorithms	F_1 (kW)	P_{loss} (%)	F_2 (kVAr)	Q_{loss} (%)
1	MFO	776.10	1.1244	572.50	1.3397
	DE	772.10	1.1186	569.70	1.3332
	HB	771.05	1.1171	569.20	1.3320
2	MFO	720.60	1.0440	533.95	1.2495
	DE	718.00	1.0402	532.25	1.2455
	HB	717.40	1.0393	532.15	1.2453
3	MFO	657.00	0.9518	493.35	1.1545
	DE	654.20	0.9478	491.55	1.1503
	HB	652.90	0.9459	490.80	1.1485
4	MFO	667.70	0.9674	499.30	1.1684
	DE	667.65	0.9672	499.15	1.1680
	HB	664.35	0.9625	497.40	1.1639

Fig. 7 (A–D) illustrates the nodal voltage magnitude of the 33-bus DIMG network at the rated load level for four Cases, analysed using the DE, MFO, and HB techniques. The data in Fig. 7 (A–D) reveals that the best voltage profile was achieved in Case 4 with the DE algorithm, whereas Case 1 with the MFO method exhibited the worst voltage profile.

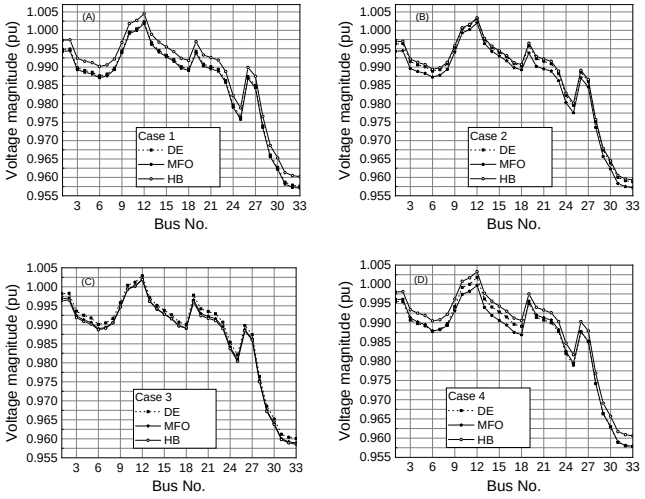

Fig. 7. Bus voltage magnitude at the rated load of cases

6. Conclusion and future work

The optimal size of three droop-based DGs to meet the electrical demand within the IEEE 33-bus IMG integrated with renewable DGs, based on the given load profile, has been determined. Analysis of the numerical results indicates that Case 3 (optimising the capacity of three DGs, including one wind turbine DG) using the honey badger algorithm results in a significant minimisation in losses power (as shown in Table 9) and an enhancement in the grid voltage magnitude. This superior performance is attributed to the HB algorithm's strong balance between global exploration and exploitation, which enables
it to escape local optima more effectively than the DE and MFO algorithms. Moreover, its adaptive foraging strategies help prevent premature convergence, resulting in more consistent and higher-quality optimal solutions in complex and nonlinear search spaces.

To enhance the penetration capacity of renewable energy in islanded microgrids, it is crucial to optimise volt-var control for smart inverter devices, including solar PV plants, STATCOM, DSATCOM, and battery storage systems. Future research should take into account the optimal allocation of these devices.

References

[1] Baran, M. E., & Wu, F. F. (1989). Network reconfiguration in distribution systems for loss reduction and load balancing. *IEEE Transactions on Power Delivery*, *4*(2), 1401–1407. https://doi.org/10.1109/61.25627

[2] Boutros, F., Doumiati, M., Olivier, J.-C., Mougharbel, I., & Kanaan, H. (2023). New modelling approach for the optimal sizing of an islanded microgrid considering economic and environmental challenges. *Energy Conversion and Management*, *277*, 116636. https://doi.org/10.1016/j.enconman.2022.116636

[3] El-Bidairi, K. S., Nguyen, H. D., Mahmoud, T. S., Jayasinghe, S. D. G., & Guerrero, J. M. (2020). Optimal sizing of Battery Energy Storage Systems for dynamic frequency control in an islanded microgrid: A case study of Flinders Island, Australia. *Energy*, *195*, 117059. https://doi.org/10.1016/j.energy.2020.117059

[4] Gupta, Y., Doolla, S., Chatterjee, K., & Pal, B. C. (2021). Optimal DG Allocation and Volt–Var Dispatch for a Droop-Based Microgrid. *IEEE Transactions on Smart Grid*, *12*(1), 169–181. https://doi.org/10.1109/TSG.2020.3017952

[5] Hameed, F., Al Hosani, M., & Zeineldin, H. H. (2019). A Modified Backward/Forward Sweep Load Flow Method for Islanded Radial Microgrids. *IEEE Transactions on Smart Grid*, *10*(1), 910–918. https://doi.org/10.1109/TSG.2017.2754551

[6] Hashim, F. A., Houssein, E. H., Hussain, K., Mabrouk, M. S., & Al-Atabany, W. (2022). Honey Badger Algorithm: New metaheuristic algorithm for solving optimization problems. *Mathematics and Computers in Simulation*, *192*, 84–110. https://doi.org/10.1016/j.matcom.2021.08.013

[7] IEEE. (2018). IEEE Standard for Interconnection and Interoperability of Distributed Energy Resources with Associated Electric Power Systems Interfaces. IEEE. https://doi.org/10.1109/IEEESTD.2018.8332112
[8] Jithendranath, J., & Das, D. (2020). Stochastic planning of islanded microgrids with uncertain multi-energy demands and renewable generations. *IET Renewable Power Generation*, *14*(19), 4179–4192. https://doi.org/10.1049/iet-rpg.2020.0889
[9] Jithendranath, J., & Das, D. (2023). Multi-Objective Optimal Power Flow in Islanded Microgrids with Solar PV Generation by NLTV-MOPSO. *IETE Journal of Research*, *69*(4), 2130–2143. https://doi.org/10.1080/03772063.2021.1886609
[10] Kerdphol, T., Fuji, K., Mitani, Y., Watanabe, M., & Qudaih, Y. (2016). Optimization of a battery energy storage system using particle swarm optimization for stand-alone microgrids. *International Journal of Electrical Power & Energy Systems*, *81*, 32–39. https://doi.org/10.1016/j.ijepes.2016.02.006
[11] Kiptoo, M. K., Lotfy, M. E., Adewuyi, O. B., Conteh, A., Howlader, A. M., & Senjyu, T. (2020). Integrated approach for optimal techno-economic planning for high renewable energy-based isolated microgrid considering cost of energy storage and demand response strategies. *Energy Conversion and Management*, *215*, 112917. https://doi.org/10.1016/j.enconman.2020.112917
[12] Krishna, P. V. N. M., Sekhar, P. C., & Behera, T. R. (2024). A robust optimal sizing of renewable-rich multi-source microgrid under uncertainties with multi-storage options. *Electrical Engineering*, *106*(5), 6547–6563. https://doi.org/10.1007/s00202-024-02331-w
[13] Kundur, P., Balu, N. J., & Lauby, M. G. (1994). *Power system stability and control*. McGraw-Hill.
[14] Liu, D., Zhang, C., Xu, Y., Dong, Z., & Chi, Y. (2023). Sensitivity Region-Based Optimization for Maximizing Renewable Generation Hosting Capacity of an Islanded Microgrid. *IEEE Transactions on Smart Grid*, *14*(4), 2496–2507. https://doi.org/10.1109/TSG.2022.3222040
[15] Liu, H., Wang, S., Liu, G., Zhang, J., & Wen, S. (2020). SARAP Algorithm of Multi-Objective Optimal Capacity Configuration for WT-PV-DE-BES Stand-Alone Microgrid. *IEEE Access*, *8*, 126825–126838. https://doi.org/10.1109/ACCESS.2020.3008553
[16] Ma, Q., Huang, X., Wang, F., Xu, C., Babaei, R., & Ahmadian, H. (2022). Optimal sizing and feasibility analysis of grid-isolated renewable hybrid microgrids: Effects of energy management controllers. *Energy*, *240*, 122503. https://doi.org/10.1016/j.energy.2021.122503
[17] Medghalchi, Z., & Taylan, O. (2023). A novel hybrid optimization framework for sizing renewable energy systems integrated with energy storage systems with solar photovoltaics, wind, battery and electrolyzer-fuel cell. *Energy Conversion and Management*, *294*, 117594. https://doi.org/10.1016/j.enconman.2023.117594
[18] Mirjalili, S. (2015). Moth-flame optimization algorithm: A novel nature-inspired heuristic paradigm. *Knowledge-Based Systems*, *89*, 228–249. https://doi.org/10.1016/j.knosys.2015.07.006
[19] Mohamed, S., Shaaban, M. F., Ismail, M., Serpedin, E., & Qaraqe, K. A. (2019). An Efficient Planning Algorithm for Hybrid Remote Microgrids. *IEEE Transactions on Sustainable Energy*, *10*(1), 257–267. https://doi.org/10.1109/TSTE.2018.2832443
[20] Nguyen, T. X., & Lis, R. (2023). Multiple Droop-Controlled DG Sites in an Islanded AC Microgrid for Power Losses Mitigation. *Automatyka, Elektryka, Zakłócenia*, *14*(3), 10–24.
[21] Nguyen, T. X., & Lis, R. (2023). Optimal size and location of dispatchable distributed generators in an autonomous microgrid using Honey Badger algorithm. *Archives of Electrical Engineering*, 871–893. https://doi.org/10.24425/aee.2023.147416
[22] Price, K. V. (1996). Differential evolution: A fast and simple numerical optimizer. *Proceedings of North American Fuzzy Information Processing*, 524–527. https://doi.org/10.1109/NAFIPS.1996.534790
[23] Roy, N. B., & Das, D. (2021). Optimal allocation of active and reactive power of dispatchable distributed generators in a droop controlled islanded microgrid considering renewable generation and load demand uncertainties. *Sustainable Energy, Grids and Networks*, *27*, 100482. https://doi.org/10.1016/j.segan.2021.100482
[24] Salman, U. T., Al-Ismail, F. S., & Khalid, M. (2020). Optimal Sizing of Battery Energy Storage for Grid-Connected and Isolated Wind-Penetrated Microgrid. *IEEE Access*, *8*, 91129–91138. https://doi.org/10.1109/ACCESS.2020.2992654
[25] Soroudi, A. (2017). *Power System Optimization Modeling in GAMS*. Springer International Publishing. https://doi.org/10.1007/978-3-319-62350-4
[26] Tomar, A. (Ed.). (2021). *Control of standalone microgrid*. Academic Press, an imprint of Elsevier.
[27] Wolpert, D. H., & Macready, W. G. (1997). No free lunch theorems for optimization. *IEEE Transactions on Evolutionary Computation*, *1*(1), 67–82. https://doi.org/10.1109/4235.585893
[28] Yazdavar, A. H., Shaaban, M. F., El-Saadany, E. F., Salama, M. M. A., & Zeineldin, H. H. (2020). Optimal Planning of Distributed Generators and Shunt Capacitors in Isolated Microgrids With Nonlinear Loads. *IEEE Transactions on Sustainable Energy*, *11*(4), 2732–2744. https://doi.org/10.1109/TSTE.2020.2973086

Ph.D. Tuan-Ho Le
e-mail: tuanhole@qnu.edu.vn

Received the B.Sc. degree in electrical engineering from University of Science and Technology – The University of Danang, Vietnam, in 2004, the M.Sc. degree in Electrical Engineering from Hanoi University of Science and Technology, Vietnam, in 2008 and the Ph.D. degree in Industrial and management systems engineering from Dong-A University, South Korea, in 2016. From 2004 to now, he is a lecturer at Faculty of Engineering and Technology, Quy Nhon University, Vietnam. Since 2016, he has been a member of the editoral board of International journal of Quality engineering and technology, from Inderscience publishers.
His research interests include AI, power system forecasting, and power system analysis and optimization.

https://orcid.org/0000-0002-9638-8171

Ph.D. Tham X. Nguyen
e-mail: nguyenxuantham@qnu.edu.vn

Received the M.Sc. degree in electrical engineering from the Quy Nhon University, Vietnam, in 2016 and the Ph.D. degree in automation, electronics, electrical engineering, and space technologies from the Faculty of Electrical Engineering, Wrocław University of Science and Technology, Poland, in 2024. He is currently a lecturer in the Faculty of Engineering and Technology, Quy Nhon University, Vietnam.
His research interests include voltage stability and control, the integration of distributed energy resources into microgrids in both grid-connected and islanded modes, and the application of optimisation methods in these areas.

https://orcid.org/0000-0001-6247-2132

Prof. Robert Lis
e-mail: robert.lis@pwr.edu.pl

Prof. dr. Robert Lis received his Ph.D. and D.Sc. (Eng.) degrees in Electrical Engineering (electric power systems) from Wroclaw University of Science and Technology (Wroclaw TECH) in 1996 and 2014, respectively. Since 1996, he has been with the Faculty of Electrical Engineering, Department of Electrical Power Engineering, at Wroclaw TECH. He became an associate professor in 2014 and has been a full professor since 2025. He leads the research team on power networks and systems.
His research interests include the analysis and modelling of electrical power systems, the integration of large numbers of decentralized renewable energy sources into electric power systems, and wide-area monitoring and control of power systems.

https://orcid.org/0000-0002-5328-5543

M.Sc. Muhammad Jamshed Abbass
e-mail: muhammad.abbass@pwr.edu.pl

Muhammad Jamshed Abbass received the M.Sc. degree in electrical engineering from Riphah International University, Islamabad. He is currently pursuing the Ph.D. degree with the Wrocław University of Science and Technology, Wroclaw, Poland. His research interests include machine learning, voltage stability within power systems, control design, analysis, the modelling of electrical power systems, the integration of numerous decentralized renewable energy sources into the electric power systems, and power system wide-area monitoring and control.

https://orcid.org/0000-0003-2831-2316